

The NA62 Experiment: Prospects for the $K^+ \rightarrow \pi^+ \nu \bar{\nu}$ Measurement

Giuseppe Ruggiero*[†]

CERN

E-mail: giuseppe.ruggiero@cern.ch

The general principles of the NA62 experiment for measuring the $K^+ \rightarrow \pi^+ \nu \bar{\nu}$ branching ratio are reviewed. The goal of the experiment is to collect about 100 events of $K^+ \rightarrow \pi^+ \nu \bar{\nu}$ in two years of data with less than 20% background. An analysis of the performances based on detailed simulations and data from various test beams shows that the sensitivity of the experiment matches the requirements. The results from the NA62 technical run of November 2012 are also reported.

*2013 Kaon Physics International Conference,
29 April-1 May 2013*

University of Michigan, Ann Arbor, Michigan - USA

*Speaker.

[†]for the NA62 Collaboration: G. Aglieri Rinella, F. Ambrosino, B. Angelucci, A. Antonelli, G. Anzivino, R. Arcidiacono, I. Azhinenko, S. Balev, A. Biagioni, C. Biino, A. Bizzeti, T. Blazek, A. Blik, B. Bloch-Devaux, V. Bolotov, V. Bonaiuto, D. Britton, G. Britvich, N. Brook, F. Bucci, V. Buescher, F. Butin, T. Capussela, V. Carassiti, N. Cartiglia, A. Cassese, A. Catinaccio, A. Ceccucci, P. Cenci, V. Cerny, C. Cerri, O. Chikilev, R. Ciaranfi, G. Collazuol, P. Cooke, P. Cooper, E. Cortina Gil, F. Costantini, A. Cotta Ramusino, D. Coward, G. D'Agostini, J. Dainton, P. Dalpiaz, H. Danielsson, N. De Simone, D. Di Filippo, L. Di Lella, N. Doble, V. Duk, V. Elsha, J. Engelfried, V. Falaleev, R. Fantechi, L. Federici, M. Fiorini, J. Fry, A. Fucci, S. Gallorini, L. Gatignon, A. Gianoli, S. Giudici, L. Glonti, F. Gonnella, E. Goudzovski, R. Guida, E. Gushchin, F. Hahn, B. Hallgren, H. Heath, F. Herman, E. Iacopini, O. Jamet, P. Jarron, K. Kampf, J. Kaplon, V. Karjavin, V. Kekelidze, A. Khudiyakov, Yu. Kiryushin, K. Kleinknecht, A. Kluge, M. Koval, V. Kozhuharov, M. Krivda, J. Kunze, G. Lamanna, C. Lazzeroni, R. Leitner, M. Lenti, E. Leonardi, P. Lichard, R. Lietava, L. Litov, D. Lomidze, A. Lonardo, N. Lurkin, D. Madigozhin, G. Maire, A. Makarov, I. Mannelli, G. Mannonchi, A. Mapelli, F. Marchetto, P. Massarotti, K. Massri, P. Matak, G. Mazza, E. Menichetti, M. Mirra, M. Misheva, N. Molokanova, M. Morel, M. Moulson, S. Movchan, D. Munday, M. Napolitano, F. Newson, A. Norton, M. Noy, G. Nuessle, V. Obraztsov, S. Padolski, R. Page, T. Pak, V. Palladino, A. Pardons, E. Pedreschi, M. Pepe, F. Petrucci, R. Piandani, M. Piccini, J. Pinzino, M. Pivanti, I. Polenkevich, I. Popov, Yu. Potrebenikov, D. Protopopescu, F. Raffaelli, M. Raggi, P. Riedler, A. Romano, P. Rubin, G. Ruggiero, V. Ryjov, A. Salamon, G. Salina, V. Samsonov, E. Santovetti, G. Saracino, F. Sargeni, S. Schifano, V. Semenov, A. Sergi, M. Serra, S. Shkarovskiy, A. Sotnikov, V. Sougonyaev, M. Sozzi, T. Spadaro, F. Spinella, R. Staley, M. Statera, P. Sutcliffe, N. Szilasi, M. Valdata-Nappi, P. Valente, B. Velghe, M. Veltri, S. Venditti, M. Vormstein, H. Wahl, R. Wanke, P. Wertelaers, A. Winhart, R. Winston, B. Wrona, O. Yushchenko, M. Zamkovsky, A. Zinchenko.

1. Introduction

Among the many rare flavour changing neutral current K and B decays, the ultra rare decays $K \rightarrow \pi \nu \bar{\nu}$ play a key role in the search for new physics through underlying mechanisms of flavour mixing. The SM branching ratio can be computed to an exceptionally high degree of precision: the $O(G_F^2)$ electroweak amplitudes exhibit a power-like GIM mechanism; the top-quark loops largely dominate the matrix element; the sub-leading charm-quark contributions have been computed at NNLO order [1]; the hadronic matrix element can be extracted from the branching ratio of the $K^+ \rightarrow \pi^0 e^+ \nu$ decay, well known experimentally [2]. The prediction for the $K^+ \rightarrow \pi^+ \nu \bar{\nu}$ channel is $(7.81 \pm 0.75 \pm 0.29) \times 10^{-11}$ [3]. The first error comes from the uncertainty on the CKM matrix elements, the second one is the pure theoretical uncertainty. This decay is one of the best probes for new physics effects complementary to the LHC, especially within non Minimal Flavour Violation models [4, 5]. Since the extreme theoretical cleanness of these decays remains also in these scenarios, even deviations from the SM value at the level of 20% can be considered signals of new physics. Also, the decay can be used for a measurement of V_{td} free from hadronic uncertainties and independently from that obtained with B mesons decays. The decay $K^+ \rightarrow \pi^+ \nu \bar{\nu}$ has been observed by the experiments E787 and E949 at the Brookhaven National Laboratory and the measured branching ratio is $1.73_{-1.05}^{+1.15} \times 10^{-10}$ [6]. Nevertheless only a measurement of the branching ratio with at least 10% accuracy can be a significant test of new physics. This is the main goal of the NA62 experiment at CERN-SPS [7].

2. Overview of the NA62 Experiment

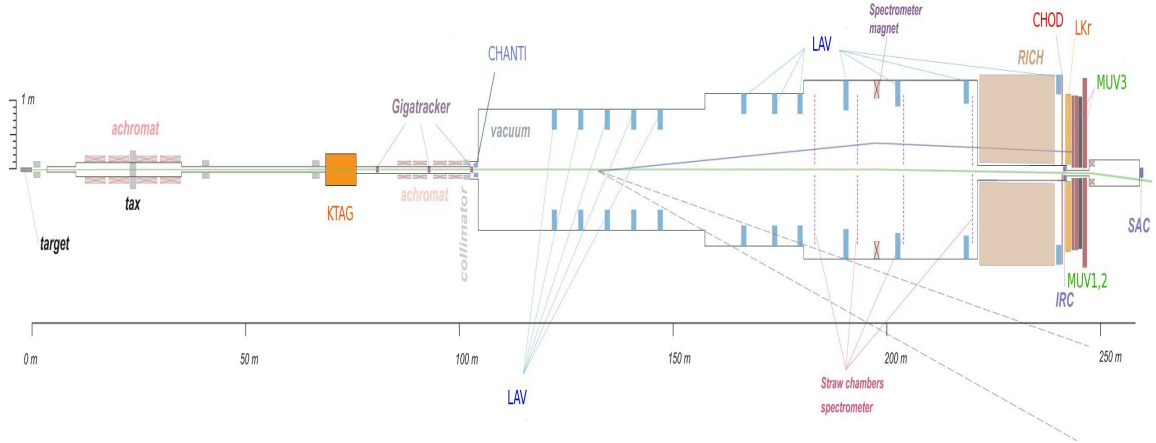
NA62 aims to collect of the order of 100 $K^+ \rightarrow \pi^+ \nu \bar{\nu}$ events in about two years of data and to keep the total systematic uncertainty smaller than the statistical one. To this purpose, at least 10^{13} K^+ decays are required, assuming a 10% signal acceptance and a $K^+ \rightarrow \pi^+ \nu \bar{\nu}$ branching ratio of 10^{-10} . The need of keeping the systematic uncertainty small, requires a rejection factor for generic kaon decays of the order of 10^{12} and the possibility to measure efficiencies and background suppression factors directly from data.

The same CERN-SPS extraction line already used by NA62 for R_K measurement [8], can deliver the required proton intensity in order to produce enough kaons. Considerations about signal acceptance drive the choice of a 75 GeV/c charged kaon beam with 1% momentum bite. As a consequence, NA62 makes use of a decay-in-flight technique to identify K^+ decay products.

The experimental setup consists of a 100 m long beam line to select the appropriate secondary beam. This beam contains π^+ (70%), protons (23%) and K^+ (6%). The rate seen by the detectors along the beam line integrated over a surface of 12.5 cm^2 is about 750 MHz. A 80 m long evacuated volume downstream the last beam line elements define the decay region. The detectors are designed to measure the secondary particles from kaon decays occurring in the decay volume. The integrated rate downstream is about 10 MHz, mainly coming from K^+ decays. Figure 1 shows the layout of the experiment. A more detailed review of the detectors has been also given at this conference [9].

3. Signal and Background

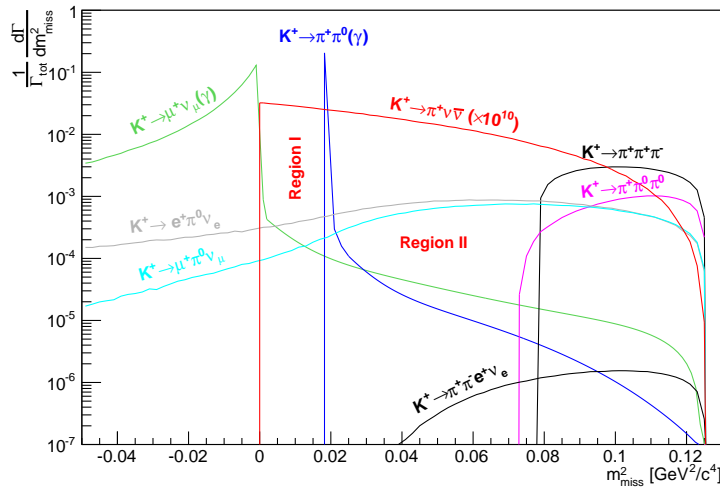
The signature of the signal is one track in the final state matched with one K^+ track in the


Figure 1: Layout of the NA62 experiment.

beam. The $m_{miss}^2 \equiv (P_K - P_{\pi^+})^2$, with P_K and P_{π^+} the four momenta of the K^+ and the charged pion, fully describes the kinematics of the decay. Backgrounds come from all the K^+ decay modes and from accidental single tracks matched with a K^+ -like track.

The distribution of the m_{miss}^2 allows a separation of the signal from the main K^+ decay modes by defining two signal regions where a minimum background is expected: region I between 0 and the $K^+ \rightarrow \pi^+ \pi^0$ peak, region II between the $K^+ \rightarrow \pi^+ \pi^0$ peak and the $K^+ \rightarrow \pi^+ \pi^+ \pi^-$ threshold (see figure 2). Nevertheless, the total background in these regions is still several order of magnitude larger than the $K^+ \rightarrow \pi^+ \nu \bar{\nu}$, as a consequence of the main decay modes leaking there via resolution effects and radiative tails, semileptonic decays and even rare decays like $K^+ \rightarrow \pi^+ \pi^- e^+ \nu$.

Possible interactions of the beam with the material along the beam line and in the residual gas in the vacuum region are the main sources for accidental single track background.


Figure 2: m_{miss}^2 distribution for signal and backgrounds from the main K^+ decay modes: The backgrounds are normalized according to their branching ratio; the signal is multiplied by a factor 10^{10} .

3.1 Strategy for a Signal Selection

The presence of one track reconstructed in the downstream spectrometer (straw chambers) matched in space and time with one track reconstructed in the beam spectrometer (Gigatracker), is the first requirement for a signal selection. A set of criteria for pion identification allows the suppression of the decay modes with muons and positrons. They involve requirements for signals in the RICH, in the forward electromagnetic calorimeter (LKr) and in the hadronic calorimeters (MUV1, MUV2 and MUV3) compatible with a single π^+ hypothesis. The same requests are also effective for controlling the backgrounds with more than one charged track in the final state. The LKr is also fundamental to suppress decay modes with photons in the final state, namely $K^+ \rightarrow \pi^+ \pi^0$, by vetoing events with clusters not associated to the π^+ . For the same reason events with signals in the photon veto system (LAVs, IRC, SAC) compatible with a γ hypothesis are rejected. A signal in the Cerenkov counter mounted on the beam line (KTAG) ensures the presence of a kaon in time with the tracks in the Gigatracker and in the spectrometer downstream. This allows the suppression of most of the accidental tracks coming from the interactions of the pions in the beam with the material along the beam line. Finally two global requirements are applied: the kaon decay has to take place in the first 60 m of the decay volume; the measured momentum of the downstream π^+ must be between 15 and 35 GeV.

3.2 Estimation of the $K^+ \rightarrow \pi^+ \pi^0(\gamma)$ background

The $K^+ \rightarrow \pi^+ \pi^0$ decay mode is primarily rejected by selecting the two signal regions defined above. The tracking system allows a $10^{-3} (\text{GeV}/c^2)^2$ resolution on the m_{miss}^2 . This gives the possibility to push the signal regions at 8σ from the $K^+ \rightarrow \pi^+ \pi^0$ peak while keeping enough signal acceptance. A detailed Monte Carlo simulation based on Geant4 [10] gives a rejection factor from kinematics of about 5×10^3 . Figure 3 shows the distribution of the reconstructed m_{miss}^2 obtained from simulation. The non gaussian tails due to the multiple scattering and the pileup in the Gigatracker are the main limiting factors to the kinematic rejection power. For what concerns the pileup, the difference of rates in the Gigatracker (750 MHz) and in the downstream detectors (10 MHz) may induce a possible wrong assignment of the K^+ track measured in the Gigatracker and the π^+ track measured downstream. As a consequence, the resolution of the m_{miss}^2 increases by a factor of 3, resulting in a loss of kinematic rejection power. The precise timing within 200 ps between the upstream and downstream track ensured by the Gigatracker, RICH and KTAG is the key ingredient to reduce the mismatching probability below the percent level, which corresponds to about one half of the total kinematic rejection inefficiency.

The photon rejection must guarantee a π^0 suppression by 8 orders of magnitude. Nevertheless the π^0 has at least 40 GeV, after requiring that the π^+ momentum should not exceed 35 GeV/c. The system of electromagnetic calorimeters and photon vetoes of NA62 ensures a geometrical coverage for photons up to 50 mrad and down to 100 MeV. About 0.2% of the $K^+ \rightarrow \pi^+ \pi^0$ have one photon outside the detection region, but the other photon has always an energy in the 10 GeV range or even more and travels in the forward direction, hitting the LKr or the small angle calorimeters (IRC and SAC). An analysis of the data taken by the NA48 experiment during a special run in 2004 [11], shows that the LKr calorimeter detects single photons above 10 GeV with an inefficiency below 10^{-5} . This measurement proves that the photon detection system of NA62 fits the requirements

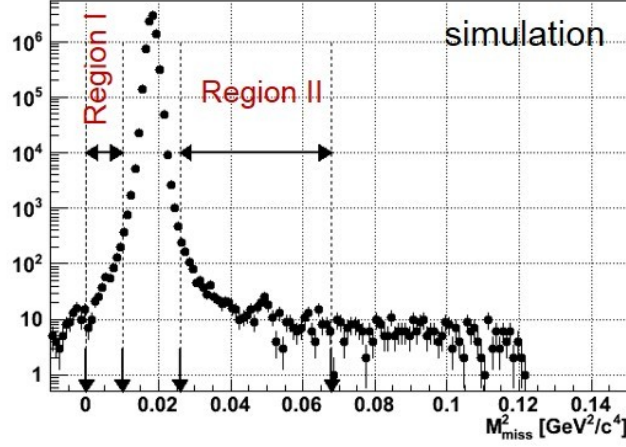


Figure 3: Distribution of the reconstructed m_{miss}^2 obtained from simulation for $K^+ \rightarrow \pi^+ \pi^0$. The events with a π^+ decay are rejected by the requirement on pion identification. The effect of the pileup on the tails is not included.

in terms of π^0 detection inefficiency. A very detailed simulation of the detector apparatus shows that the material in front of the LKr calorimeter (the RICH detectors and the 20 m long beam pipe connecting the end of the downstream spectrometer to the entrance window of the LKr itself) gives a negligible contribution to the single photon detection inefficiency, allowing the calorimeter to recover the photons even after catastrophic interactions in this region. On the other hand this material limits the detection inefficiency of the small angle calorimeters (IRC and SAC) at the level of 10^{-4} to 10^{-3} . Nevertheless this inefficiency remains small enough to keep the overall photon rejection within the specifications.

The kinematic rejection power and the π^0 detection inefficiency evaluated both from simulation and measurements on data, have been factorized out and combined with the geometrical acceptance. A cut and count analysis, without any optimization, applied on simulation suggests a 10% residual background coming from $K^+ \rightarrow \pi^+ \pi^0$. An additional 3% contribution comes from the radiative tails, as estimated from dedicated Monte Carlo studies. Samples of $K^+ \rightarrow \pi^+ \pi^0$ selected using only the calorimetric information or only the tracking information allow direct measurements on data of the kinematic rejection power and of the photon detection inefficiency. The strong dependence of the residual background on the momentum of the π^+ and on the Z coordinate of the decay vertex can also be used for further optimization.

3.3 Estimation of the $K^+ \rightarrow \mu^+ \nu$ background

Because of the pion hypothesis, the m_{miss}^2 spectrum of the $K^+ \rightarrow \mu^+ \nu$ is negative and momentum dependent: it approaches zero at increasing pion momenta. As a consequence, the cuts on the m_{miss}^2 defining the signal regions allow a strong suppression of this background. Also, the cut at 35 GeV/c on the maximum track momentum enhances the kinematic rejection factor. The situation is very close to the case of $K^+ \rightarrow \pi^+ \pi^0$, with the difference that the $K^+ \rightarrow \mu^+ \nu$ background affects

mainly region I and the muon does not suffer from hadronic elastic scattering. The distribution of the reconstructed m_{miss}^2 obtained from simulation is shown in figure 4 (left). The overall rejection factor is 1.5×10^4 with the limiting factors coming from the multiple scattering non gaussian tails and from the pileup in the Gigatracker.

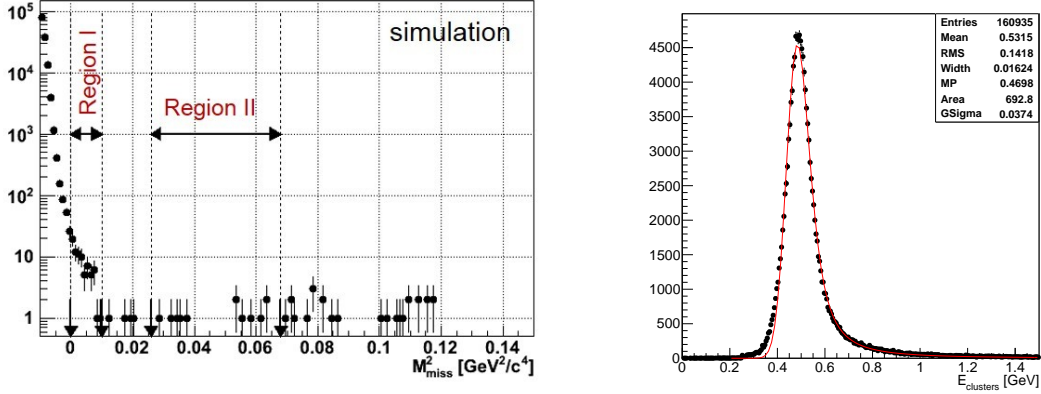


Figure 4: Distribution of the reconstructed m_{miss}^2 obtained from simulation for $K^+ \rightarrow \mu^+ \nu$ (left). The cut on the track momentum is applied. The effect of the pileup on the tails is not included. Energy release of MIP particles in the LKr reconstructed from data taken during the 2012 technical run of NA62 (right). The fit of the energy distribution to a Landau function is superimposed.

The muon suppression comes from the pion identification which makes use of calorimetric and Cerenkov information. The LKr is able to discriminate electromagnetic and hadronic clusters and to produce a clear signature for MIP particles, as shown from the analysis of the data collected during the NA62 technical run of November 2012 (see figure 4 (right)). These inputs are combined with those from the hadronic calorimeter made up by the MUV1, MUV2 and MUV3 subdetectors. The ultimate inefficiency of the muon-pion separation is 10^{-5} and comes from the absorption of the muons in the material in front of the MUV3 due to the energy loss via Brehmsstrahlung. A dedicated test beam in 2009 showed that the RICH of NA62 allows a muon-pion separation with a sub-percent inefficiency, by keeping the cut on the maximum momentum at 35 GeV and on the minimum at 15 GeV because of the pion Cerenkov threshold of the Neon (the RICH radiator). Also this test measured a time resolution of the RICH below 100 ps [12].

The rejection inefficiencies from kinematics, calorimetry and RICH can be factorized out and combined with the geometrical acceptance, giving a residual background from $K^+ \rightarrow \mu^+ \nu$ at the level of 2.2%. Another percent contribution comes from the radiative tail. The combined use of two independent methods for muon suppression, like the RICH and the calorimeters, allows a powerful cross-check of the inefficiencies of the two techniques separately. Also the RICH can be used to check the momentum measured in the spectrometer, by assuming the mass of the pions.

3.4 Estimation of the $K^+ \rightarrow \pi^+ \pi^+ \pi^-$ background

The requirement of having only one track reconstructed in the straw chambers rejects about 99% of the $K^+ \rightarrow \pi^+ \pi^+ \pi^-$. The m_{miss}^2 spectrum is crucial to strongly suppress the contribution

from those $K^+ \rightarrow \pi^+ \pi^+ \pi^-$ with one π^+ and the π^- not reconstructed in the spectrometer. Also the cut at 15 GeV/c on the minimum track momentum is effective to this goal. The overall rejection factor from kinematics is 1.5×10^6 , as estimated from simulation. The residual background comes from events entering in region II (see figure 5), mainly, because of the tails of the reconstructed m_{miss}^2 due to the non gaussian multiple scattering. The effect from the pileup in the Gigatracker, instead, is marginal.

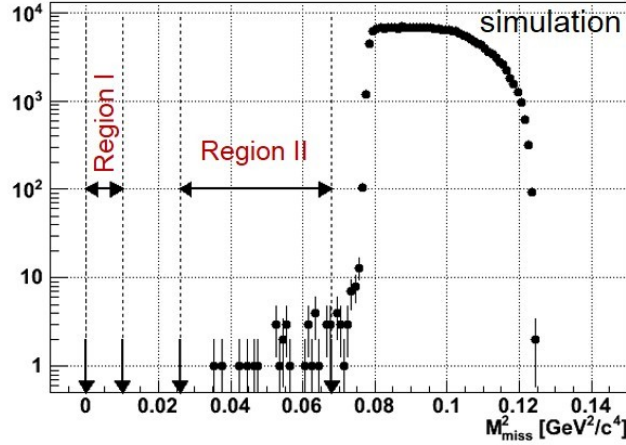


Figure 5: Distribution of the reconstructed m_{miss}^2 from simulation for $K^+ \rightarrow \pi^+ \pi^+ \pi^-$ after the one track requirement. The effect of the pileup on the tails is not included.

The largest part of the remaining events have one good π^+ reconstructed in the straw chambers and the other two charged pions pointing in the beam hole of the first and second straw chambers. Nevertheless, the strength of the magnetic field of the spectrometer magnet after the second chamber and the distance between this magnet and the detectors downstream are such to ensure a full geometrical coverage downstream the magnet for the detection of the π^- up to 65 GeV/c. Also the two straw chambers downstream of the magnet are slightly offset in the bending plane on the side of the deflection of the positive particles, just to enhance the probability of detecting negative particles already in the straw chambers themselves. The following detectors are employed for rejecting the residual $K^+ \rightarrow \pi^+ \pi^+ \pi^-$: the RICH to detect the π^- s with an energy larger than 15 GeV; the LKr, MUV1 and MUV2 to detect the π^- without energy constraints; the scintillators array after the RICH (CHOD) and the LKr to detect also the products of the nuclear interactions of the π^- , if any; the last station of the large angle veto after the RICH, mainly for detecting μ^- escaping at large angle in case of low energy π^- decays; extra segments in the straw chambers for detecting the π^- itself and those π^+ hitting at least two chambers before going undetected downstream. Taking into account the correlations between the detectors, the overall rejection factor is of the order of 10^6 .

The kinematic cuts and the multiplicity cuts can be factorized out with good approximation. A simple cut and count analysis on simulation shows a residual contribution from $K^+ \rightarrow \pi^+ \pi^+ \pi^-$ at the level of 1-2%. The use of several different methods for detecting the π^- gives the possibility to cross-checks the inefficiency of π^- rejection directly on data. A similar analysis suggests a

contribution to the background from the rare $K^+ \rightarrow \pi^+ \pi^- e^+ \nu$ decay below 2%.

3.5 Background from Beam Interactions

The main source from accidental background comes from the interactions of the beam in the material along the beam line, namely the Gigatracker stations (about $1.5 X_0$ in total) and the residual gas in the vacuum region. The KTAG is critical for the rejection of these accidentals. During the NA62 technical run of 2012 a time resolution of the KTAG better than 100 ps was measured with less than 1% pion mistagging. This ensures the suppression of almost all the background coming from the interactions of the π^+ and protons of the beam (about 94%).

The interactions with the residual gas have been simulated with Fluka [13] and the products of the interactions propagated in the main simulation of NA62. This background turns out to be negligible after taking into account the measured time resolution of the KTAG and scaling the level of vacuum in the decay region achieved during the 2012 technical run with a partial set of vacuum pumps (2×10^{-5} mbar) to the final set of pumps foreseen for the 2014.

The nuclear interactions of the K^+ in the last station of the Gigatracker are the other main source of accidentals that can mimic a π^+ signal in the detectors downstream. A suppression factor greater than 10^3 comes from the kinematic constraint on the reconstructed vertex. The detection of the other particles coming out from the nuclear interactions gives another 10^5 rejection factor, at least. This high level of suppression is enforced by the 35 GeV/c cut on the π^+ maximum momentum, leaving at least 40 GeV of additional energy to be detected. The main detectors for this goal are a guard ring around the last station of the Gigatracker (CHANTI), the LAVs' and the forward calorimeters. The ultimate background comes from the charge exchange processes, like $K^+ n \rightarrow K_L p$ with a subsequent $K_L \rightarrow e^- \pi^+ \nu$, where the additional energy may go undetected because the e^- misses the detector acceptance.

The background induced by beam interactions shows a strong dependence with the longitudinal reconstructed vertex position, allowing a direct monitor on data.

3.6 Results from Signal and Background Studies

Table 1 summarizes the results about the sensitivity of NA62 for the measurement of the $K^+ \rightarrow \pi^+ \nu \bar{\nu}$. The results are based on a cut and count analysis without any optimization. The number of events are normalized to 4.5×10^{12} expected number of kaons decays per year of data. The SM $K^+ \rightarrow \pi^+ \nu \bar{\nu}$ branching ratio is assumed. The branching ratios for the background decay modes are taken from PDG [14].

4. Results from the 2012 Technical Run

NA62 took data in November 2012 during a technical run with a partial detector configuration. The goal of this run was: commissioning of the final beam line; analysis of the time and spatial correlation between subdetectors and estimation of their time resolution and efficiency. The detectors installed were: KTAG on the beam line with 50% of readout channels; 1 plane of one straw chamber; CHOD; LKr with 30% of readout channels; MUV2 and MUV3.

The beam line provided a charged secondary beam of 75 GeV/c. A selection based on the information from the electromagnetic calorimeter identified a sample of $K^+ \rightarrow \pi^+ \pi^0$ events. The

Decay	event/year
$K^+ \rightarrow \pi^+ \nu \bar{\nu}$	45
$K^+ \rightarrow \pi^+ \pi^0$	5
$K^+ \rightarrow \pi^+ \pi^+ \pi^-$	1
$K^+ \rightarrow \pi^+ \pi^- e^+ \nu$	<1
$K^+ \rightarrow \pi^+ \pi^0 \gamma (IB)$	<1
$K^+ \rightarrow \mu^+ \nu \gamma (IB)$	1.5
other rare decays	0.5
Total backgrounds	<10

Table 1: Signal and background from K^+ decays estimated from the sensitivity studies. The numbers are normalized to the 4.5×10^{12} expected number of kaons decays per year of data. The SM branching ratio is assumed for the signal.

cluster shape in the LKr tags the electromagnetic-like clusters. The position and energy of these clusters and the knowledge of the nominal direction of the beam allow the determination of the decay vertex, under the hypothesis that the two clusters belong to photons from a π^0 decay. The knowledge of the vertex position provides the determination of the four-momenta of the photons and of the π^0 . Under the hypothesis of $K^+ \rightarrow \pi^+ \pi^0$ event, the four momentum of the π^+ follows from energy conservation. As a consequence of these assumptions the quantity $m_{miss}^2 \equiv (P_K - P_{\pi^0})$ corresponds to $m_{\pi^+}^2$ for $K^+ \rightarrow \pi^+ \pi^0$ events. Figure 6 (left) shows the m_{miss}^2 as selected from data. The peak of the $m_{\pi^+}^2$ is clearly visible. The background is mainly due to $K^+ \rightarrow \pi^+ \pi^0 \gamma$, $K^+ \rightarrow \pi^+ \pi^0 \pi^0$, $K^+ \rightarrow \pi^0 e^+ \nu$, $K^+ \rightarrow \pi^0 \mu^+ \nu$ and $K^+ \rightarrow \pi^+ \pi^0$ with the charged pion (or accidental) cluster mis-identified as a photon cluster. The events show a clear correlation in time with signals in KTAG coming from the K^+ (150 ps time resolution), hits in CHOD coming from the π^+ (<400 ps time resolution) and signals in MUV3 in case of π^+ decay or punch-through from the MUV2 (450 ps time resolution). The KTAG inefficiency is about 87%, corresponding to 95% for a fully instrumented detector. Most of the background is rejected by exploiting the spatial and time correlation between the subdetectors (see figure 6 right). The peak corresponds to the $m_{\pi^+}^2$ within the uncertainty coming from the energy calibration of the LKr. The resolution is about 3.8×10^{-3} (GeV/c²)². The residual background is at the percent level.

The analysis performed during the technical run does not make any use of information from a tracking system. Therefore this method will be used to measure on data the tails of the kinematic variables reconstructed with the tracking devices.

5. Conclusions

The sensitivity of the NA62 experiment has been reviewed by using detailed simulations and inputs from test beams. The results match the requirements of the experiment both in terms of signal statistics and background. A technical run of NA62 with the final beam line and a partial detector setup took place in November 2012. The analysis of the data shows that the performances of the beam line and the time resolution and the inefficiency of the detectors fit the expectations.

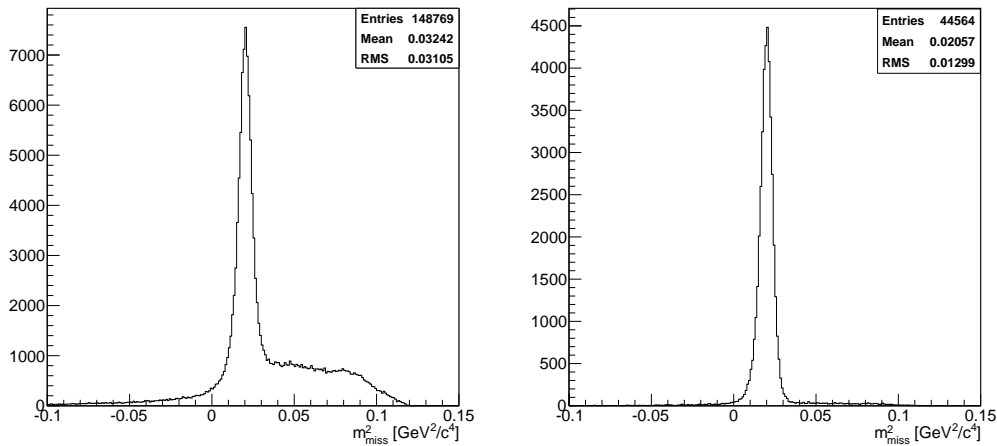


Figure 6: Distribution of the m_{miss}^2 after using the information from the LKr only (left); after exploiting the time and spatial correlations between the detectors (right).

References

- [1] A. J. Buras, M. Gorbahn, U. Haisch and U. Nierste, JHEP **0611** (2006) 002.
- [2] C. Amsler *et al.*, Phys. Lett. **B667** (2008) 1.
- [3] J. Brod, M. Gorbahn and E. Stamou, Phys. Rev. D **83** (2011) 034030.
- [4] G. Isidori, F. Mescia, P. Paradisi, C. Smith and S. Trine, JHEP **0608** (2006) 064.
- [5] M. Blanke, A. J. Buras, B. Duling, S. Recksiegel and C. Tarantino, Acta Phys. Polon. B **41** (2010) 657.
- [6] A. V. Artamonov *et al.* [BNL-E949 Collaboration], Phys. Rev. D **79** (2009) 092004.
- [7] NA62 Technical Design Document, NA62-10-07; <https://cdsweb.cern.ch/record/14049857>.
- [8] C. Lazzeroni *et al.* [NA62 Collaboration], Phys. Lett. B **719** (2013) 326.
- [9] F. Hahn, this conference, PoS(KAON13) 031.
- [10] S. Agostinelli *et al.* [GEANT4 Collaboration], Nucl. Instrum. Meth. A **506** (2003) 250.
- [11] NA62 Collaboration, CERN-SPSC-2007-035, SPSC-M-760;
- [12] B. Angelucci *et al.*, Nucl. Instrum. Meth. A **621** (2010) 205.
- [13] A. Ferrari, P.R. Sala, A. Fasso and J. Ranft, CERN-2005-010.
- [14] J. Beringer *et al.* (Particle Data Group), Phys. Rev. **D86** (2012) 010001.